The 2018 World Congress on
Advances in Civil, Environmental, & Materials Research (ACEM18)
Songdo Convensia, Incheon, Korea, August 27 - 31, 2018

Structural and Magnetic Phase Transition in BFO Nanoparticles – Role of Calcination Temperature

M Tahir[1)*], Attia Awan[1)], Saira Riaz[2)], S Sajjad Hussain[2)], Zohra N Kayani[2)], and Shahzad Naseem[2)]

[1), 2)] *Centre of Excellence in Solid State Physics, Punjab University, Lahore, Pakistan*

[*] *tahirmesp1207@gmail.com*

ABSTRACT

Among various multiferroics, bismuth iron oxide (BFO, $BiFeO_3$) is currently known as the only material that exhibit ferromagnetic and ferroelectric behavior at room temperature. As compared to the bulk, low dimensional BFO exhibits extra ordinary different properties. Such advanced properties arise because of the enhancement of surface area along with the development of energy states. On the other hand, high value of leakage current and week ferromagnetism are the two limitations that still need to be addressed. In the present study, BFO nanoparticles are synthesized using low cost sol-gel method. Chemically synthesized nanoparticles are calcined at 300˚C, 400 ºC, 500 ºC and 600 ºC. X-ray diffraction (XRD) results show amorphous nature for nanoparticles calcined at 300 ºC. Transition from amorphous to crystalline phase pure $BiFeO_3$ is observed at calcination temperature of 400˚C. Nanoparticles calcined at temperature of 500 ºC and 600 ºC result in $Bi_2Fe_4O_9$ and $BiFeO_3$ mixed phases. Nanoparticles with calcination temperature of 300 ºC, 500 ºC and 600 ºC result in weak magnetic behavior. Strong ferromagnetic behavior with saturation magnetization of 0.027emu is obtained at calcination temperature of 400 ºC.

1. INTRODUCTION

Multiferroics belongs to the class of materials that exhibit any two of the four ferroic orders simultaneously. The four multiferroic orders are:1) ferrotoroidic; 2) ferroelastic; 3) ferroelectric; and 4) ferromagnetic. Some multiferroic materials exhibit the effect known as “magnetoelectric effect” i.e. coupling between ferromagnetic and ferroelectric order exist over a range of temperature (Dhanalakshmi et al. 2017; Kolte et al. 2017; Shi et al. 2016; Catalano et al. 2016). Name “multiferroics” was think up by Hans Schmid (Schmid 1994) due to contrary nature of prerequisites required for ferromagnetism and ferroelectricity to exist in the same material. These materials have offered their advantages in various applications including quantum electromagnets, spin valves, transducers, capacitors, multistate memories and many more (Schmid 1994; Agbelele et al. 2017, Xu et al. 2017).

Among various multiferroics, bismuth iron oxide (BFO, $BiFeO_3$) is currently known as the only material that exhibit ferromagnetic and ferroelectric behavior at room temperature and magnetoelectric coupling between the two properties. It possesses ferroelectric perovskite structure that is rhombohedrally distorted with Curie

---

[1)] Graduate Student
[2)] Professor

temperature of 1100K. It belongs to R3c space group. It exhibit G-type antiferromagnetic behavior with high Neel temperature of 643K. BFO is known to have spiral spin structure with long range periodicity of 62nm. The propagation of this spiral spin wave is along $[110]_{hex}$ direction. In addition, FeO_6 octahedron in BFO exhibits antiferrodistortive clockwise-anticlockwise tilt along $[001]_{hex}$ direction. This direction of tilt is equivalent to three fold pseudo cubic direction ($[111]_{cub}$). Therefore, BFO belonging to R3c space group have an additional parameter i.e. θ. It is the measure of antiferrodistortive tilt in BFO (Jeong et al. 2011; Ruette et al. 2004).

Two main phase transitions are observed in crystal structure of BFO: 1) Ferroelectric Transition: Transition from ferroelectric perovskite structure to cubic phase with space group $Pm\bar{3}m$. This transition takes place at Curie temperature of 1100K; 2) Magnetic Transition: From G-type antiferromagnetic behavior to paramagnetic behavior at Neel temperature of 643K. In addition, there is a third phase transition associated with θ. At high temperatures, thermal energy breaks the antiferrodistortive ordering along $[111]_{cub}$ direction (Jeong et al. 2011; Ruette et al. 2004; Smolenskii et al. 1982).

Despite the advantages of BFO, the biggest problem related to BFO is its antiferromagnetic or weak magnetic ordering at room temperature. In addition, magnetic ordering is also lost in BFO due to volatile nature of bismuth (Riaz et al. 2015; Riaz et al. 2014a,b). For overcoming this difficulty, we here report effect of post thermal calcination treatment on BFO nanoparticles synthesized through sol-gel method. Changes in magnetic properties are interconnected with variation in calcination temperature.

2. Experimental Details

Low cost and application oriented sol-gel method was adopted for synthesis of BFO nanoparticles. Iron nitrate and bismuth nitrates were used as precursor for sol synthesis. In the first step of sol synthesis, iron nitrate was dissolved in ethylene glycol and stirring was done at room temperature. In the second step, bismuth nitrate was dissolved in ethylene glycol while stirred at room temperature. In third stage, two solutions, made in step one and two, were mixed together. The resultant solution was treated thermally on hot plate at 80 ºC to obtain BFO sol. BFO sol was heated at 100 ºC to obtain BFO nanoparticles. These nanoparticles were calcined at 300-600 ºC (interval 100 ºC).

Calcined BFO nanoparticles were studied for their structural evaluation with the help of Bruker D8 Advance X-ray Diffractometer (XRD). Magnetic analysis was performed using Lakeshore's 7407 Vibrating Sample Magnetometer.

3. Results and Discussion

Fig. 1 shows XRD patterns for BFO nanoparticles calcined at temperature range of 300-600 ºC. Nanoparticles calcined at 300 ºC (Fig. 1(a)) were amorphous in nature as no diffraction peak was observed. Presence and splitting of planes (104) and (110) indicated formation of phase pure perovskite structure of $BiFeO_3$ at 400 ºC (Fig. 1(b)). Peaks are indexed using JCPDS card 86-1518. No peaks related to bismuth deficient or rich phases were observed. When these BFO nanoparticles were calcined at 500 ºC

(Fig. 1(c)) inclusion of $Bi_2Fe_4O_9$ phase was observed along with $BiFeO_3$. This indicates that at calcination temperature of 500 ºC volatility of bismuth oxide takes place thus, leading to incorporation of $Bi_2Fe_4O_9$ phase in $BiFeO_3$. Also reduction in crystallinity was observed at 500 ºC indicated by decrease in peak intensities. When these nanoparticles were calcined at 600 ºC (Fig. 1(d)) drastic reduction in crystallinity was observed along with presence of $BiFeO_3$ and $Bi_2Fe_4O_9$ phases.

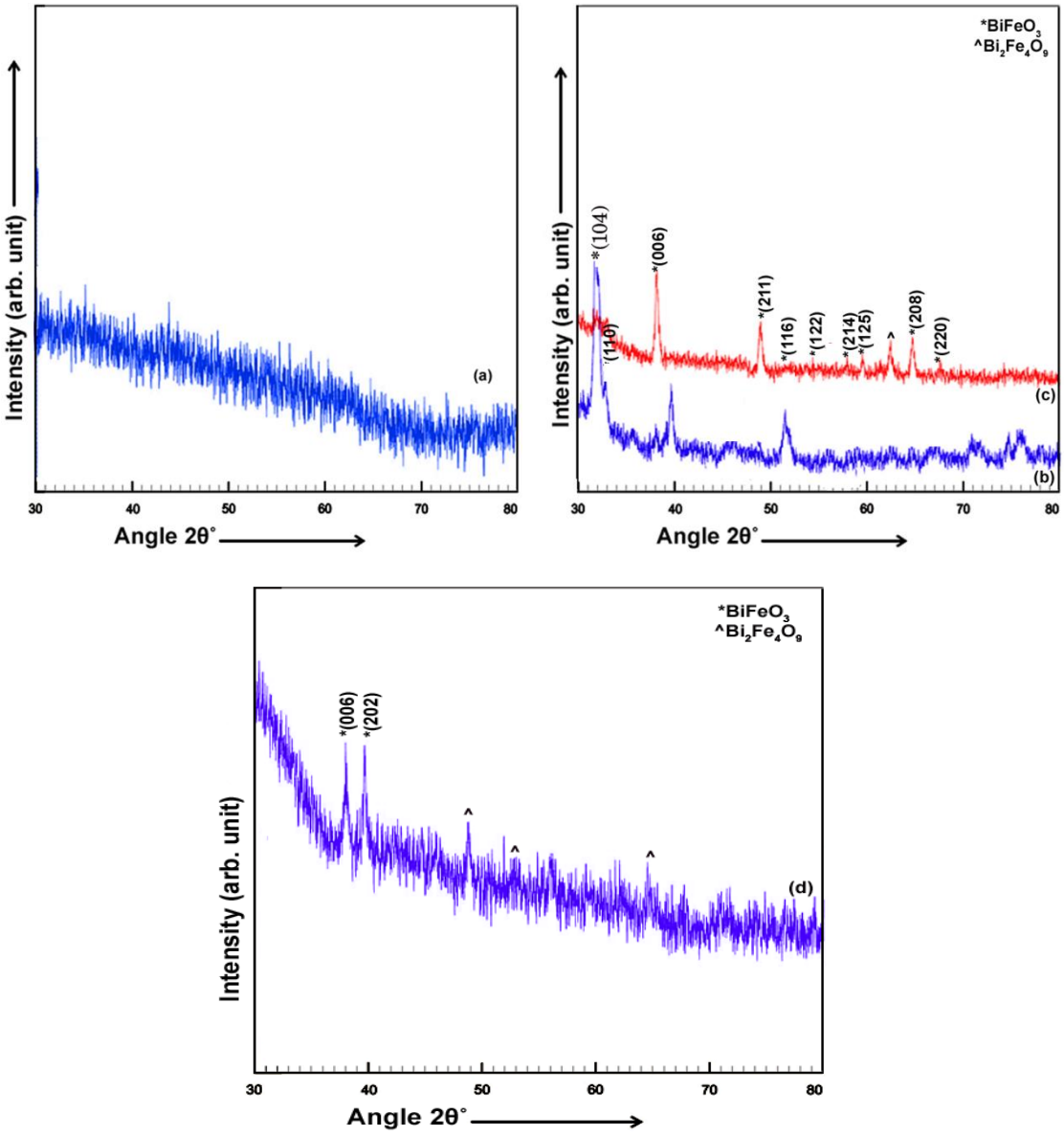

Fig. 1. XRD patterns for BFO nanoparticles calcined at (a) 300 ºC; (b) 400 ºC; (c) 500 ºC and (d) 600 ºC.

Crystallite size (t) (Culity 1956), dislocation density (δ) (Riaz et al. 2014) and lattice parameters (*a*,*c*) (Culity 1956) were calculated using equations (1)-(3).

$$t = \frac{0.9\lambda}{B\cos\theta} \tag{1}$$

$$\delta = \frac{1}{t^2} \tag{2}$$

$$\frac{1}{d_{hkl}^2} = \frac{4}{3}\left(\frac{h^2 + hhk + k^2}{a^2}\right) + \frac{l^2}{c^2} \tag{3}$$

Where, λ is the wavelength used i.e. 1.5406Å, B is full width at half maximum, θ is diffraction angle and (hkl) are miller indices. Crystallite size (Table 1) of 16nm was calculated for nanoparticles calcined at temperature of 400ºC. While, crystallite size for nanoparticles calcined at temperature of 500ºC and 600ºC was observed as 22nm and 24nm. Increase in crystallite size at calcination temperature is associated with reduction in Gibb's free energy of particles with temperature. In case of supersaturated solutions reduction in Gibb's free energy occurs through segregation of solute. After initial nucleation, growth of species decreases. And this process continues till equilibrium has been achieved. This drop in Gibb's free energy is balanced by rise in surface energy. For formation of nuclei with radii "r" the relation between chemical potential (ΔG) and Gibb's free energy (ΔG_v) per unit volume is represented by Equation (4) (Dhir et al. 2017).

$$\Delta G = \frac{4\pi r^3 \Delta G_v}{3} + 4\pi r^2 \gamma \tag{4}$$

Where, γ represents surface energy per unit area. Driving force behind nucleation and growth of particles is reduction in Gibb's free energy. For a given temperature (T), Gibb's free energy is given in Equation (5) (Dhir et al. 2017).

$$\Delta G_v = -\frac{kT}{\Omega}\ln\frac{C}{C_o} \tag{5}$$

Where, C is the concentration of solute, Ω represents the atomic value. Equation (5) indicates that reduction in Gibb's free energy occurs through increase in temperature thus, resulting in increase in crystallite size (Dhir et al. 2017).

Table 1. Structural parameters for BFO nanoparticles.

Calcination temperature (ºC)	Phase	Crystallite size (nm)	Dislocation density (10^{15}lines/m^2)	Lattice parameters (Å)		Unit cell volume (Å)
				a	c	
300	Amorphous	---	---	---	---	---
400	$BiFeO_3$	16	3.90625	5.578	13.869	373.69
500	$Bi_2Fe_4O_9$+$BiFeO_3$	22	2.06612	5.532	13.856	367.21
600	$Bi_2Fe_4O_9$+$BiFeO_3$	24	1.73611	5.500	13.849	362.79

Lattice parameters (Table 1) for BFO nanoparticles calcined at temperature of 400˚C is equal to lattice JCPDS card no. 86-1518. Reduction in lattice parameter and unit cell volume at calcination temperature 500 ºC and 600 ºC is associated with presence of mix $Bi_2Fe_4O_9$ and $BiFeO_3$ phases as observed in Fig. 1(c) and (d).

Magnetic hysteresis curves for BFO nanoparticles can be observed in Fig. 2. Nanoparticles calcined at 300 ºC (Fig. 2(a)) exhibit weak magnetic behavior indicated by presence of open hysteresis at low field strength (Fig. 2(a) inset). Transition to strong ferromagnetic behavior was observed for phase pure $BiFeO_3$ at calcination temperature 400 ºC (Fig. 2(b)). At high calcination temperature of 500 ºC and 600 ºC (Fig. 2(c,d)) weak magnetic behavior was observed due to presence of mix $BiFeO_3$ and $Bi_2Fe_4O_9$ phases.

Bulk $BiFeO_3$ is antiferromagnetic in nature. Within each (111) layer in the crystal structure, ferromagnetic ordering occurs in Fe^{3+} cations. Between adjacent (111) layers, antiferromagnetic ordering arises. Each Fe^{3+} cation is bounded by six adjacent Fe^{3+} cations. These six Fe^{3+} cations have spins parallel to each other but antiparallel to the spin of the Fe^{3+} cation that is surrounded. Two antiferromagnetic orderings of G-type behavior are then possible: 1) Magnetic moments of Fe^{3+} cations are collinear with (111) plane and thus belong to magnetic group Bb(m); 2) Magnetic moments are collinear to [111] direction and thus, belong to magnetic group 3m (Kalinkin et al. 2010; Tirupathi et al. 2014).

Previously, studies regarding neutron diffraction have revealed that structure of BFO is composed of cycloidal spin with period of 62nm. The appearance of spin modulation in non-centrosymmetric crystals is due to size effect. If the size of nanoparticles falls below the cycloid spin structure of BFO then ferromagnetic behavior is induced in otherwise antiferromagnetic BFO(Shah et al. 2014a,b; Majid et al. 2015; Kalinkin et al. 2010; Tirupathi et al. 2014). Phase purity (Fig. 1(b)) and reduced crystallite size (~16nm; Table 1) resulted in strong ferromagnetic behavior of BFO nanoparticles calcined at 400 ºC.

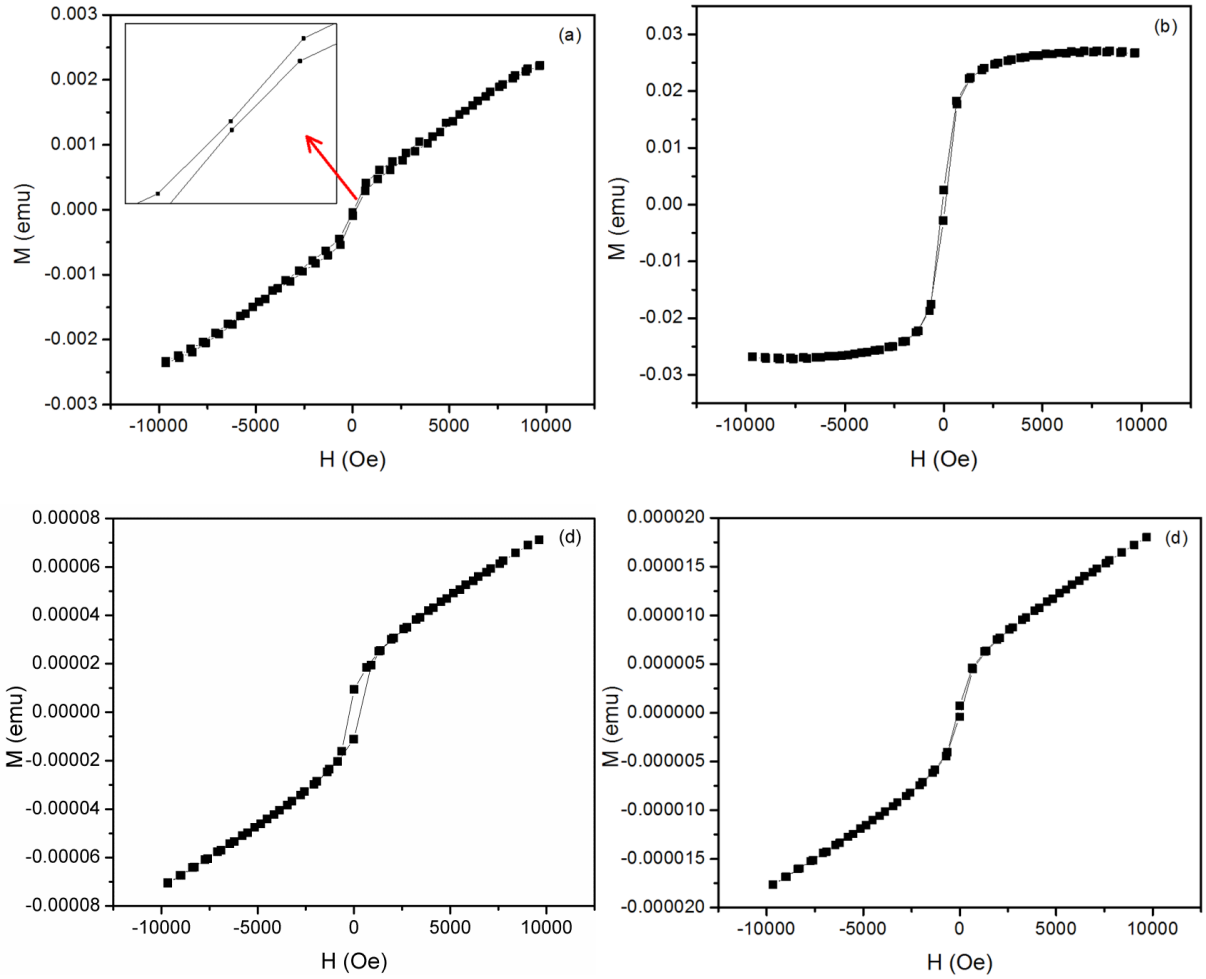

Fig. 2. M-H curves for BFO nanoparticles calcined at (a) 300 ºC; (b) 400 ºC; (c) 500 ºC and (d) 600 ºC.

4. Conclusions

BFO nanoparticles, synthesized using sol-gel method, were calcined at 300-600˚C (interval 100˚C). XRD results show amorphous behavior for nanoparticles calcined at 300˚C. Highly crystalline $BiFeO_3$ phase was obtained for nanoparticles which were calcined at temperature of 400˚C. Mixed phases of $BiFeO_3$ and $Bi_2Fe_4O_9$ were

observed for nanoparticles which were calcined at 500˚C and 600˚C. Weak magnetic behavior, with open hysteresis at low field strength was studied for nanoparticles calcined at temperature of 300˚C. Strong ferromagnetic behavior (saturation magnetization of 0.027emu) was recorded for nanoparticles with the calcination temperature of 400˚C. Weak magnetic behavior at 500˚C and 600˚C is attributed to mix $BiFeO_3$ and $Bi_2Fe_4O_9$ phases.

REFERENCES

Agbelele, A, Sando, D., Toulouse, C., Paillard, C., Johnson, R.D., Rüffer, R., Popkov, A.F., Carrétéro, C, Rovillain, P., Le Breton, J.M., Dkhil, B., Cazayous, M., Gallais, Y., Méasson, M.A., Sacuto, A., Manuel, P., Zvezdin, A.K., Barthélémy, A., Juraszek, J., and Bibes, M., (2017), "Strain and Magnetic Field Induced Spin-Structure Transitions in Multiferroic $BiFeO_3$" *Adv. Mater*. **29,** 1602327.

Catalano, M.R., Spedalotto, G., Condorelli, G.G., and Malandrino, G. (2016), "MOCVD Growth of Perovskite Multiferroic $BiFeO_3$ Films: The Effect of Doping at the A and/or B Sites on the Structural, Morphological and Ferroelectric Properties" *Adv. Mater. Int*. **4**(8) ,1601025

Cullity, B.D. (1956), "Elements of x-ray diffraction," Addison Wesley Publishing Company, USA.

Dhanalakshmi, B., Kollu, P., Sekhar, B.C., Rao, B.P., and Rao, P.S.V.S. (2017), "Enhanced magnetic and magnetoelectric properties of Mn doped multiferroic ceramics" *Ceram. Int.,* **43** (12), 9272-9275.

Dhir, G., Uniyal, P., and N.K., Verma (2017), "Tactics of particle size for enhanced multiferroic properties in nanoscale Ca-doped $BiFeO_3$" *Phys. Status Solidi C* **14**(5)*,*1600253.

Gao, R., Fu, C., Cai, W., Chen, G., Deng, X., and Cao X. (2017), "Thickness Dependence of Photovoltaic Effect in BiFeO3 Thin Films Based on Asymmetric Structures" *J. Electron. Mater.* **46**, 2373–2378.

Gitanjali, D., Poonam, U., and Verma N.K. (2014), "Effect of Particle Size on Magnetic and Dielectric Properties of Nanoscale Dy-Doped $BiFeO_3$ " *J. Supercond. Nov. Magn.,* **27**,1569–1577.

Jeong, Y.K., Bark, C.W., Ryu, S., Lee, J.H., and Jang, H.M. (2011), "R3c-R3m octahedron-tilting transition in rhombohedrally-distorted $BiFeO_3$ multiferroics" *J. Korean Phys. Soc.,* **58 ,**810-820.

Kalinkin, A.N., and Skorikov, V.M., (2017), "$BiFeO_3$ films and single crystals as a promising inorganic material for spintronics" *J. Inorg. Chem.* **55**, 1794–1809.

Kolte, J., Daryapurkar, A.S., Agarwal, M., Gulwade, D.D., and Gopalan P. (2017), "Magnetoelectric properties of microwave sintered $BiFeO_3$ and $Bi_{0.90}La_{0.10}Fe_{0.95}Mn_{0.05}O_3$ nanoceramics "*Mater. Chem. Phys.* **193,** 253-259.

Lomanova, N.A., Tomkovich, M.V., Sokolov, V.V., Ugolkov, V.L., Panchuk, V.V., Semenov, V.G., Pleshakov, I.V., Volkov, M.P., and Gusarov, V.V. (2018), "Thermal and magnetic behavior of $BiFeO_3$ nanoparticles prepared by glycine-nitrate combustion," *J. Nanopart. Res.*, **20**(2), 17-25.

Majid, F., Riaz, S., and Naseem, S. (2015), "Microwave-assisted sol–gel synthesis of $BiFeO_3$ nanoparticles," *J. Sol-Gel Sci. Technol.* **74**, 329-339.

Riaz, S., Majid, F., Shah, S.M.H., and Naseem, S. (2014a), "Enhanced magnetic and structural properties of Ca doped $BiFeO_3$ thin films," *Indian J. Phys.* **88**, 1037–1044.

Riaz, S., Shah, S.M.H., Akbar, A., Atiq, S., and Naseem, S. (2015), "Effect of Mn doping on structural, dielectric and magnetic properties of $BiFeO_3$ thin films," *J. Sol-Gel Sci. Technol.,* **74**, 310-319.

Riaz, S., Shah, S.M.H., Akbar, A., Kayani, Z.N., and Naseem, S. (2014b) "Effect of Bi/Fe Ratio on the Structural and Magnetic Properties of $BiFeO_3$ Thin Films by SolGel," *IEEE Trans. Magn.,* **50**, 2201304.

Ruette, B, Zvyagin, S, Pyatakov, A.P., Bush, A., Li, J.F., Belotelov, V.I., Zvezdin, A.K., and Viehland D. (2004) "Magnetic-field-induced phase transition in $BiFeO_3$ observed by high-field electron spin resonance:Cycloidal to homogeneous spin order" *Phys. Rev. B* **69**, 064114.

Schmid, H. (1994), "Multi-ferroic magnetoelectrics" *Ferroelectrics* **162**, 317-338.

Shah, S.M.H, Akbar, A., Riaz, S., Atiq, S., and Naseem, S. (2014a), "Magnetic, Structural, and Dielectric Properties of $Bi_{1-x}K_xFeO_3$ Thin Films Using Sol-Gel," *IEEE Trans. Magn.,* **50**, 2201004

Shah, S.M.H., Riaz, S., Akbar, A., Atiq, S., and Naseem, S. (2014b), "Effect of Solvents on the Ferromagnetic Behavior of Undoped BiFeO3 Prepared by Sol-Gel," *IEEE Trans. Magn*., **50**, 2200904.

Shi, X.X, Liu, X.Q., and Chen, X.M. (2017). "Readdressing of Magnetoelectric Effect in Bulk $BiFeO_3$" *Adv. Funct. Mater*.**27**(12), 1604037.

Smolenskii, G.A., and Chupis, I.E. (1982), "Ferroelectromagnets," *Sov. Phys. Usp.* **25**,475-490.

Tirupathi P., Mandal S.K., and Chandra A., (2015), "Effect of oxygen annealing on the multiferroic properties of Ca^{2+} doped $BiFeO_3$ nanoceramics" *J. Appl. Phys.* **116**, 244105.

Xu Q., Hu C., Wang J., and Du, J., (2017), "Enhanced ferromagnetism in $BiFeO_3$ powders by rapid combustion of graphite Powders" *AIP Adv.* **7,** 055803.